

See discussions, stats, and author profiles for this publication at: <https://www.researchgate.net/publication/234163139>

Synchrotron radiation X-ray absorption spectroscopic studies in solution and electrochemistry of a nitroimidazole conjugated heteroscorpionate copper (II) complex

ARTICLE *in* POLYHEDRON · NOVEMBER 2012

Impact Factor: 2.01 · DOI: 10.1016/j.poly.2012.08.073

CITATIONS

4

READS

19

6 AUTHORS, INCLUDING:



Marco Giorgetti

University of Bologna

85 PUBLICATIONS 1,262 CITATIONS

SEE PROFILE



Alberto Zanelli

Italian National Research Council

68 PUBLICATIONS 1,044 CITATIONS

SEE PROFILE



Maura Pellei

University of Camerino

106 PUBLICATIONS 2,034 CITATIONS

SEE PROFILE



Carlo Santini

University of Camerino

121 PUBLICATIONS 2,313 CITATIONS

SEE PROFILE



Synchrotron radiation X-ray absorption spectroscopic studies in solution and electrochemistry of a nitroimidazole conjugated heteroscorpionate copper(II) complex

Marco Giorgetti ^{a,*}, Silvia Tonelli ^a, Alberto Zanelli ^b, Giuliana Aquilanti ^c, Maura Pellei ^d, Carlo Santini ^d

^a Dipartimento di Chimica Fisica ed Inorganica, Università di Bologna, INSTM UdR Bologna, Viale del Risorgimento 4, 40136 Bologna, Italy

^b CNR, ISOF, Via Gobetti 101, 40129 Bologna, Italy

^c Sincrotrone Trieste S.C.p.A., S.S. 14 Km 163.5, 34149 Basovizza, Trieste, Italy

^d School of Science and Technology, Chemistry Section, Università di Camerino, via S. Agostino 1, 62032 Camerino (MC), Italy

ARTICLE INFO

Article history:

Received 10 May 2012

Accepted 28 August 2012

Available online 7 September 2012
September 2012

Keywords:

Copper(II)

Scorpionates

EXAFS

XANES

Cyclic voltammetry

ABSTRACT

Synchrotron radiation X-ray absorption spectroscopy has been used to determine the solution structure of the nitroimidazole conjugated heteroscorpionate copper(II) complex $\{[(L^{MN})_2Cu]Cl_2\}$ (L^{MN} = 2,2-bis(3,5-dimethyl-1H-pyrazol-1-yl)-N-(2-(2-methyl-5-nitro-1H-imidazol-1-yl)ethyl)acetamide) at three different pH values. The strategy used for the XAS data analysis for a straightforward data interpretation is presented. The copper center is coordinated by two molecules of ligands, describing a quasi-octahedral figure, in all investigated solutions, demonstrating the stability of the complex in solution. The copper complex displays a pH dependence where the Cu–O first shell distance (from the carbonyl) lengthens at acid pH; the Cu–N equatorial distances are almost the same. XANES spectroscopy also indicates structural rearrangements occurring in solution at various pH, where the spectrum at pH 4.4 displays the largest differences from the other ones. The cyclic voltammetry curves obtained on the same solutions show an irreversible peak due to the reduction of Cu(II) \rightarrow Cu(I), which falls at potential of about 0.4–0.5 V versus SCE, and it is found to be depending on pH. The potentiality of the joint XAS and electrochemical approach in the determination of the structural characteristics of the solutions is highlighted.

© 2012 Elsevier Ltd. All rights reserved.

1. Introduction

Heteroscorpionate ligands of general formula $[RR'C(az)_2]$ (az = azolyl groups; $R = H$ or az) bearing organic functional groups (R') on the bridging carbon have attracted considerable attention and their coordination chemistry towards main group and transition metals has been extensively studied [1–5]. The first acetamido and thioacetamido heteroscorpionate ligands were prepared by Otero et al. [6,7]. Bis(3,5-dialkylpyrazol-1-yl)acetic acids [8,9] are a convenient starting material for linker modified ligands [10]. Complexes containing these ligands have been of considerable interest owing to their important use as metalloenzyme models relevant to biochemistry [11–18] and metal-based antitumor drugs [19].

During the last decade, the interest of this research group has focused in the synthesis of new heteroscorpionate ligands with pyrazole, triazole, 2-mercaptopyridine or 2-mercaptoimidazole rings [19–28]. In addition, as part of our ongoing research efforts in the design and development of radiometal-based anticancer

agents, the ^{64}Cu -labelled complexes of $[HC(CO_2)(pz^{Me2})_2Cu(thp)_2]$ and $[HC(CO_2)(tz)_2Cu(thp)_2]$, (thp = tris(hydroxymethyl)phosphine) have been prepared to evaluate their usefulness as PET radiopharmaceuticals [29].

Nitroimidazoles are a class of hypoxia tracer that have been extensively investigated for hypoxia-selective cytotoxicity and hypoxic cell radiosensitization *in vitro* and *in vivo* [30]. It has been shown that nitroimidazoles can be trapped in cells with low pO_2 values [31], and the 2-nitroimidazole compounds such as the $[^{18}F]$ fluoromisonidazole [32–35] or 2-nitroimidazole cyclam derivatives radiolabelled with ^{99m}Tc , ^{64}Cu and ^{67}Cu [36] have been used for PET imaging of stroke, myocardium ischemia and tumor hypoxia as potential PET/SPECT agents for tumor hypoxia. 4-Nitroimidazole-based thioflavin-T derivatives were radiolabelled with iodine-131 and showed *in vitro* binding to viable hypoxic or aerobic tumor cells [37], while nitroimidazole conjugates of bis(thiosemicarbazone)copper(II) recently showed additive or synergistic selectivity for tumor hypoxia compared to their individual components [38].

In a recent work [39], we reported the synthesis and characterization of two nitroimidazole and glucosamine conjugated heteroscorpionate ligands and the related copper(II) complexes as well as

* Corresponding author. Tel.: +39 051 2093 666; fax: +39 051 2093 690.

E-mail address: marco.giorgetti@unibo.it (M. Giorgetti).

a brief investigation of their biological activity. In particular, copper complexes and the corresponding uncoordinated ligands were evaluated for their cytotoxic activity towards a panel of several human tumour cell lines. The X-ray Absorption Spectroscopy (XAS) has been used to probe the local structure of the two copper(II) complexes in the solid state [39], underlying the reliability of the approach while no X-ray diffraction data is available due to poor crystalline sample. In order to acquire structural data in the solution state, we present here a XAS study of the nitroimidazole heteroscorpionate Cu(II) complex on solutions at different pHs. As demonstrated several times, the XAS is very helpful in this context because it probes the local structure around a selected atom regardless the state of matter. Therefore, structural information in a range of 3–5 Å around the metal centre could be retrieved in disordered systems [40], amorphous inorganic materials [41], solutions [42] and biological systems [43]. For example, a study on copper(I) inorganic samples in both solid and liquid state has permitted the detection of Cu–Cu coordination [44]. Also, the solution structure of $\text{Cu}(\text{aq})^{2+}$ ion has been investigated by using full multiple-scattering analysis of the copper K-edge X-ray absorption spectrum [45]. Our group studied the XAS spectra of a series of Fe [46] and Cu [26,47] complexes of scorpionate ligands. In particular, the EXAFS probe has permitted to check the fivefold geometry of the Cu(I) complex with the bis(1,2,4-triazol-1-yl)acetate ligands. Recently, we have studied the copper coordination core in a series of Cu(II) complexes with N,S-donor macrocyclic ligands [48].

2. Experimental

2.1. Materials and general methods

The 2,2-bis(3,5-dimethyl-1H-pyrazol-1-yl)-N-(2-(2-methyl-5-nitro-1H-imidazol-1-yl)ethyl)acetamide ligand (L^{MN}) and the related Cu(II) complex $\{[(\text{L}^{\text{MN}})_2\text{Cu}]\text{Cl}_2\}$ were prepared by literature method [39]. Three solutions for XAS measurements were prepared: double distilled water, 0.1 M acetate buffer ($\text{CH}_3\text{COOH}/\text{CH}_3\text{COONa}$) and 0.1 M borate buffer (sodium tetraborate/ HCl). The obtained pH values were 6.50, 4.40 and 8.54, respectively. The concentration of the complex was 0.01 M in all solutions. XAS measurements were carried out using a suitable cell for solution which has been adapted to the XAFS beamline at ELETTRA synchrotron radiation laboratory. The cell contains about 200–500 μL of solution and uses Kapton (polyimide, cas 25036-53-7, DuPont) windows.

2.2. Electrochemistry

Electrochemical experiments have been performed at 25 °C, after Ar purging, with an AMEL 5000 electrochemical system. Cyclic voltammeteries (CVs) in water, Milli RO 15 water purification system, 0.5 $\mu\text{S cm}^{-1}$, and 0.02 M acetate buffer or borate buffers, has been carried out in a home-made glass cell with 2 mm diameter glassy carbon working electrode, aqueous KCl Saturated Calomel Electrode (SCE) and Pt wire counter-electrode in a separate compartment.

2.3. XAS experiments

XAS experiments were performed at ELETTRA Synchrotron Light Laboratory, in Basovizza (Italy), at the XAFS beam line [49]. The storage ring operated at 2.0 GeV in top up mode with a typical current of 300 mA. The data were recorded at Cu K-edge in transmission mode using ionization chamber filled with a mixture of Ar and N_2 gas in order to have 20%, 80%, and 95% of absorbing in the I0, I1, I2 chambers, respectively. Spectra were collected with a constant

k -step of 0.03 \AA^{-1} with 3 s/point acquisition time from 8750 eV to 9830 eV. Three to four spectra were collected and averaged to improve statistics. An internal reference of copper foil was used for energy calibration in each scan. This allowed a continuous monitoring of the energy during consecutive scans. The energies were defined by assigning to 8980.3 eV the first inflection point of the spectrum of the metallic copper. No energy drifts of the monochromator were observed during the experiments. The white beam was monochromatized using a fixed exit monochromator equipped with a pair of Si(111) crystals. Harmonics were rejected by using the cutoff of the reflectivity of the Platinum mirror placed at 3 mrad with respect to the beam upstream the monochromator and by detuning the second crystal (of the monochromator) by 30%.

2.4. XAS data analysis

The EXAFS analysis has been performed by using the GNXAS package [50,51] that takes into account Multiple Scattering (MS) theory. The method is based on the decomposition of the EXAFS signals into a sum of several contributions, that are the n -body terms. It allows the direct comparison of the raw experimental data with a model theoretical signal. The procedure avoids any filtering of the data and allows a statistical analysis of the results. The theoretical signal is calculated *ab-initio* and contains the relevant two-body $\gamma^{(2)}$ and the three-body $\gamma^{(3)}$ multiple scattering (MS) terms. The contribution from four-body $\gamma^{(4)}$ terms [52] has been checked out, but it was found to be negligible in this case. The phase shifts for the photoabsorber and backscatterer atoms were calculated *ab-initio* using the structural model indicated in Ref. [39], in the muffin-tin approximation. The Hedin–Lundqvist complex potential [53] was used for the exchange-correlation potential of the excited state. The core hole lifetime, Γ_c , was fixed to the tabulated value [54] and included in the phase shift calculation.

Referring to Fig. 1 and the sketch of Table 1, the n -body terms included in the fitting procedures are: the two-atom contributions $\gamma_1^{(2)}$ Cu–N1 with degeneracy of four, the two-atom contributions $\gamma_2^{(2)}$ Cu–O with degeneracy of two, the two-atom contributions $\gamma_3^{(2)}$ Cu–C with degeneracy of two, and four additional three-body contributions $\eta^{(3)}$ due to the multiple scattering of the pyrazolyl ring. In particular, the three-body contribution $\eta_1^{(3)}$ Cu–N1–N2 with degeneracy of four (four pyrazolyl rings per Cu), the three-body contribution $\eta_2^{(3)}$ Cu–N1–C5 with degeneracy of four, the three-body contribution $\eta_3^{(3)}$ Cu–N1...C3 with degeneracy of four, and the three-body contribution $\eta_4^{(3)}$ Cu–N1...C4 with degeneracy of four. It is noteworthy that the inclusion of the three-body term $\eta^{(3)}$ allows monitoring the shells beyond the first one by using the

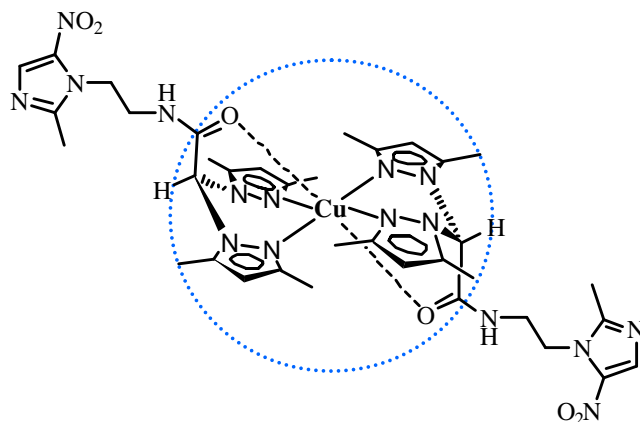
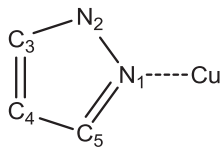
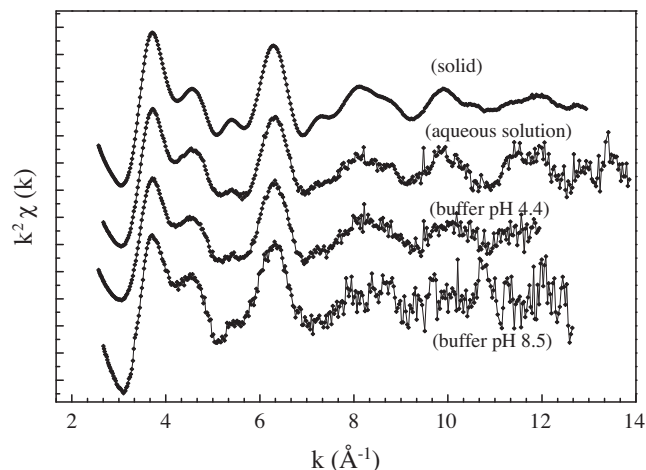


Fig. 1. Structure of the investigated complex $\{[(\text{L}^{\text{MN}})_2\text{Cu}]\text{Cl}_2\}$. The circle evidences the local atomic structure probed by EXAFS.

Table 1Selected atomic distances of the pyrazolyl rings of the ligand L^{MN} (Å) from XRD.

		
Bond length (Å)	Ring 1	Ring 2
N1–N2	1.375	1.372
N1–C5	1.359	1.357
N1...C3	2.131	2.123
N1...C4	2.164	2.160

**Fig. 2.** k^2 extracted experimental EXAFS signals at the copper K-edge of the complex $\{[(L^{MN})_2Cu]Cl_2\}$ in the solid state, and in the three buffered solutions.

same three-atom coordinates both for the two-atom and the three-atom contributions. For instance, the three-body signal $\eta^{(3)} Cu-N1-C5$ includes both $\gamma^{(2)} Cu-C5$ and $\gamma^{(3)} Cu-N1-C5$ contributions. Data analysis has been performed by minimizing a χ^2 -like function that compares the theoretical model to the experimental signal. The experimental resolution used in the fitting analysis was about 2 eV, in agreement with the stated value for the beamline used [49]. The E_0 value was found to be displaced by several eV with respect to the edge inflection point (see Table 2). The values of S_0^2 lie in the 0.97–0.99 range. The total number of parameters taken into account in the fitting procedure (including the structural and non-structural terms E_0 , S_0^2 and the experimental resolution) is 30, whereas the number of floating variable (fitting) was found to be 13. Besides, it is worth mentioning that in all cases the number of fitting parameters does not exceed the estimated 'number of independent data points' $N_{ind} = (2\delta k\delta R/\pi) + 2$, ensuring that the fit is well determined and does not lead to parameters with very large errors, thus confirming the reliability of the minimization.

3. Results

3.1. EXAFS

Fig. 1 displays the structure of the investigated complex in the solid state, which local structure has been determined by EXAFS [39]. The copper(II) ion interacts within two molecule of ligands, describing, in the solid state, a pseudo-octahedral environment where the four Cu–N equatorial distances have been quoted 2.024 Å and the two axial Cu–O bond lengths which have been quoted 2.032 Å. Hence, there is a tetragonal distortion of the CuN_4O_2 octahedron in the solid state.

To gain a complete understanding of the molecular structure of the complex, solution studies at three different pH have been done. Fig. 2 displays the comparison of the solid state and solutions experimental EXAFS spectra and the corresponding Fourier Trans-

Table 2EXAFS best-fitting results of $\{[(L^{MN})_2Cu]Cl_2\}$ in solution at different pHs. The estimated parameter errors are indicated in parentheses. Angles θ_1 , θ_2 , θ_3 , θ_4 were kept fixed to the crystallographic values of the XRD characterization of the L^{MN} ligand, while the corresponding angle Debye–Waller factor were left to float.

Bond length (degeneracy) Debye–Waller factor	Powder ^b	Aqueous solution	pH 8.5	pH 4.4
Cu–N1 (Å) (4)	2.024(7)	2.022(7)	2.01(1)	2.016(15)
σ^2 (Å ²)	0.005(2)	0.005(1)	0.005(2)	0.006(1)
Cu–O (Å) (2)	2.328(15)	2.34(2)	2.29(3)	2.38(2)
σ^2 (Å ²)	0.017(5)	0.011(4)	0.022(5)	0.018(5)
Cu–C (Å) (2)	3.16(2)	3.12(3)	3.12(4)	3.12(3)
σ^2 (Å ²)	0.003(2)	0.005(3)	0.004(2)	0.017(5)
Cu–N1–N2 (deg) (4)	120 FIX	120 FIX	120 FIX	120 FIX
σ^2 (deg ²)	24(10)	34(15)	21(10)	53(20)
Cu–N1–C5 (deg) (4)	129 FIX	129 FIX	129 FIX	129 FIX
σ^2 (deg ²)	25(15)	44(20)	17(15)	32(20)
Cu–N1...C3 (deg) (4)	157 FIX	157 FIX	157 FIX	157 FIX
σ^2 (deg ²)	70(20)	70(30)	69(30)	68(30)
Cu–N1...C4 (deg) (4)	166 FIX	166 FIX	166 FIX	166 FIX
σ^2 (deg ²)	70(30)	69(30)	70(30)	70(30)
Cu...N2 (Å); σ^2 (Å ²)	2.95; 0.008	2.97 ^a ; 0.013	2.96 ^a ; 0.013	2.94 ^a ; 0.013
Cu...C5 (Å); σ^2 (Å ²)	3.01; 0.01	3.02 ^a ; 0.014	3.01 ^a ; 0.014	3.01 ^a ; 0.019
Cu...C3 (Å); σ^2 (Å ²)	4.20; 0.018	4.21 ^a ; 0.029	4.19 ^a ; 0.024	4.19 ^a ; 0.022
Cu...C4 (Å); σ^2 (Å ²)	4.23; 0.017	4.26 ^a ; 0.014	4.25 ^a ; 0.015	4.22 ^a ; 0.015
E_0	8988.8(6)	8989.6(5)	8989.0(7)	8988(1)
S_0^2	0.99(4)	0.98(3)	0.99(4)	0.97(4)

^a Data obtained from the three body configuration (using Cu–N–N(C) angle and N(C)–N distances).^b From Ref. [39].

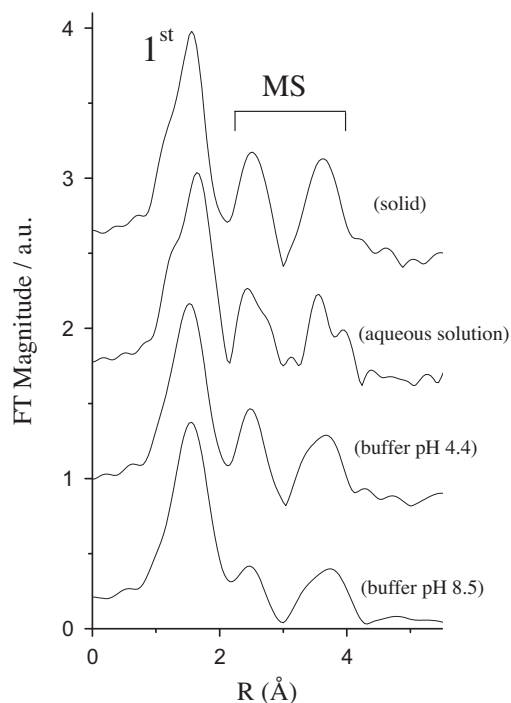


Fig. 3. Corresponding Fourier transform signal of the k^2 extracted experimental EXAFS reported in Fig. 2.

form signals are reported in Fig. 3. The EXAFS spectra of solutions are rather similar to that of the solid state, and hence no dramatic changes are expected in the local atomic environment of copper. An increase of the experimental noise is observed in solution, especially at high pH buffer. All signals are characterized by a main fre-

quency superimposed to higher frequency oscillations, with the main frequency due to the first coordination shell around the copper.

As expected, the FTs of Fig. 3, which is a pseudo radial distribution function, display a main peak in all spectra due to the Cu–N first shell interaction and other contributions, due to photoelectron multiple scattering of the pyrazolyl rings arising which causes a large multiple scattering (MS) event. In Fig. 3 all sets of peaks are similar in intensity and position demonstrating firstly the stability of the complex once dissolved at a certain pH. This means basically that the copper pseudo-octahedral geometry is retained in solutions, where each Cu(II) ion interacts with two molecules of ligands. Further, the relative high intensity of the MS contribution at 2–4 Å which is still present in the solution spectra, suggests that the scattering contribution of the ring of the scorpionate ligands is not negligible. Therefore this contribution has to be included in the fitting procedure.

In order to minimize the number of parameters used in the fit without losing any structural details carried out by the EXAFS signals, we have used an approximation concerning the atomic distances of the pyrazolyl ring. Table 1 summarizes the bond lengths of the pyrazolyl rings, as reported by XRD data of the free ligand [39]. These distances in the solid are very close each other, and hence they can be considered fixed and grouped when analyzing the EXAFS spectrum in the solid state. This approach was successfully in the analysis of $[(L^{MN})_2Cu]Cl_2$ in the solid state.

Here, taking into account the experimental evidences of Figs. 2 and 3 we can extend the consideration concerning the pyrazolyl ring distances also to the solution spectra. Hence, the subsequent fitting analysis of the EXAFS spectra will be done by considering the distances associated to the pyrazolyl ring fixed to the values quoted by the crystallography. This approximation permits handling a lower number of floating variable during the fitting procedure and to consider all the three body contributions around 4 Å around the photo-absorber. The EXAFS analysis on spectra at different pH have been done considering the structural model de-

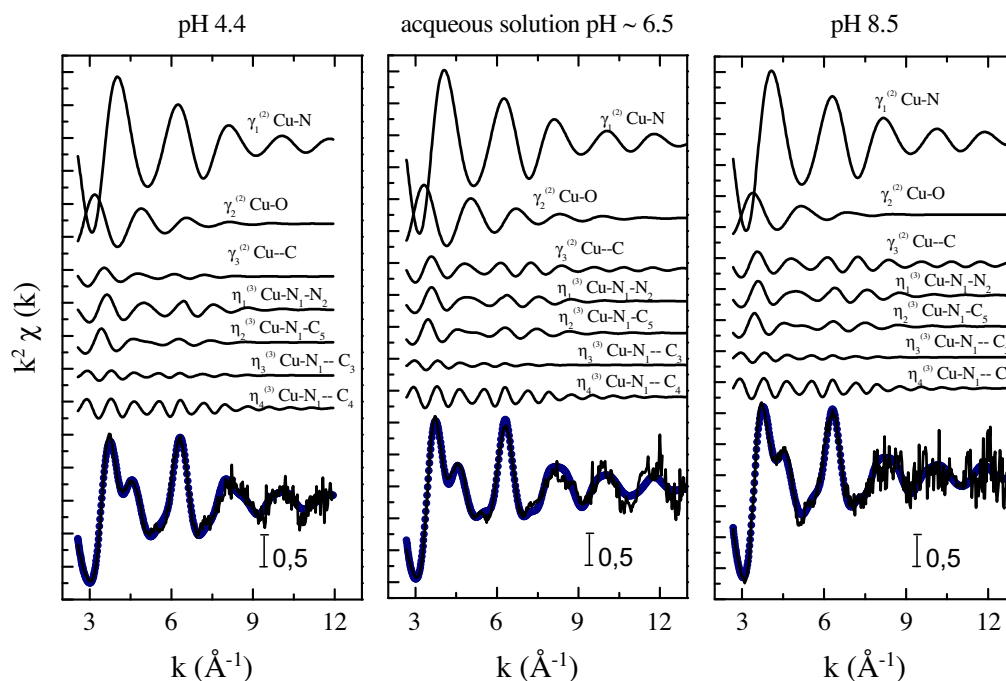


Fig. 4. Details of the EXAFS analysis of the Cu K-edge of the complex in solution at three different pHs. Each panel of the figure shows the individual EXAFS contributions, in terms of two-body and three-body signals, to the total theoretical signal. The comparison of the total theoretical signal (–) with the experimental one (···) is also reported at the bottom of each panel.

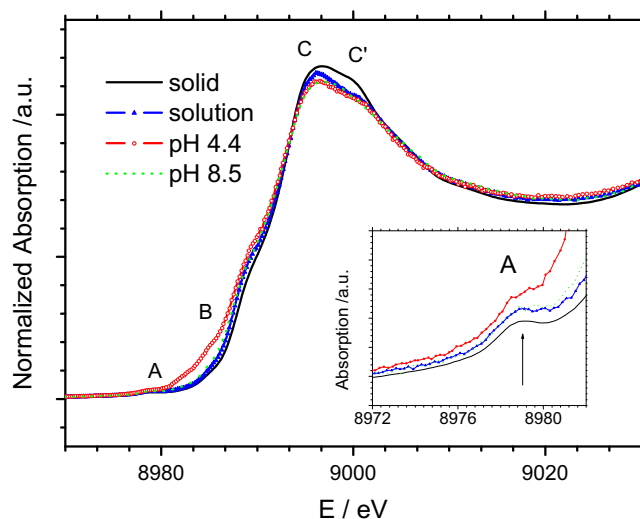


Fig. 5. Normalized XANES spectra at the Cu K-edge of the complex $\{[(L^{MN})_2Cu]Cl_2\}$ in the solid state and in different pHs solutions. The pre-edge features A is assigned to the 1s–3d transition, peak B to the 1s–4p + SD one. The inset displays a magnification of the pre-edge peak.

picted in Fig. 1 and the procedure is described in full detail in Section 2. A preliminary analysis procedure has been done in order to check the number of ligands involved in the complexation in solution. The fitting test, done for the first shell only in all experimental spectra, has unambiguously led to two units of ligands in the copper complex. The EXAFS best-fit result in detail for the three solutions, in terms of various contributions to the theoretical signals and the comparison of the total theoretical signal with the experimental one, is presented in Fig. 4.

The comparison of the theoretical and experimental signal in each panel (at the bottom) justifies the correctness of the present procedure and the accuracy of the used structural model. From the single contributions, it is evident in Fig. 4 from the figure that the Cu–N first shell is the most higher signal, as expected, but all

signal are rather important in the determination of the total theoretical one. We also remind that the four three-body signals, $\eta^{(3)}$, are almost constant in shape in all panels, because they are defined by the structural parameters which have been kept fix to the values of Table 1 and to the angles normally quoted in this class of compounds. Table 2 lists the inter-atomic distances and the corresponding EXAFS Debye–Waller factor (best-fit) of all solutions, together with their associate errors. They were determined by correlation maps (contour plots) for each pair of parameters. Examples of contour plot are available as supplementary content.

3.2. XANES

Additional information concerning the copper coordination site in the studied solutions as well as on copper effective charge could be gained by comparison of the XANES spectra, which are displayed in Fig. 5. All spectra are rather similar, and hence we expected no dramatic changes of the copper complex geometry in solutions at different pH. As Cu(II) is concerned, all spectra display a small pre-edge peak A due to the 1s–3d transition which is dipole forbidden but quadrupole allowed [55]. The inset of the figure shows a magnification of such a transition which occurs at about 8970.0 eV, being consistent with Cu(II) assignment [56]. This peak increases in intensity when solutions are concerned, and the highest one is observed at acidic pH values.

In addition, spectra displays a shoulder appearing along the rising edge (B), and the edge maximum (C and C'). The shoulder, formed by a couple of contributions, has been previously assigned [57] to a 1s–4p and 1s–4p with concurrent ligand-to-metal charge transfer (LMCT) which gains intensity because of the final state relaxation [58]. These features shift to lower energies in the case of acidic solution. The edge maximum split in two main peaks (C and C'), as observed in case of several Cu(II) complexes. These peaks are due to multiple scattering effects being dependent on the local geometric arrangement rather than on the electronic structure of copper. Theoretically, it has been proposed that a double electronic absorption channel has to be considered for reproducing the experimental spectra [59,60], and it works for several cases. This fact poses a limit for the use of the main absorption

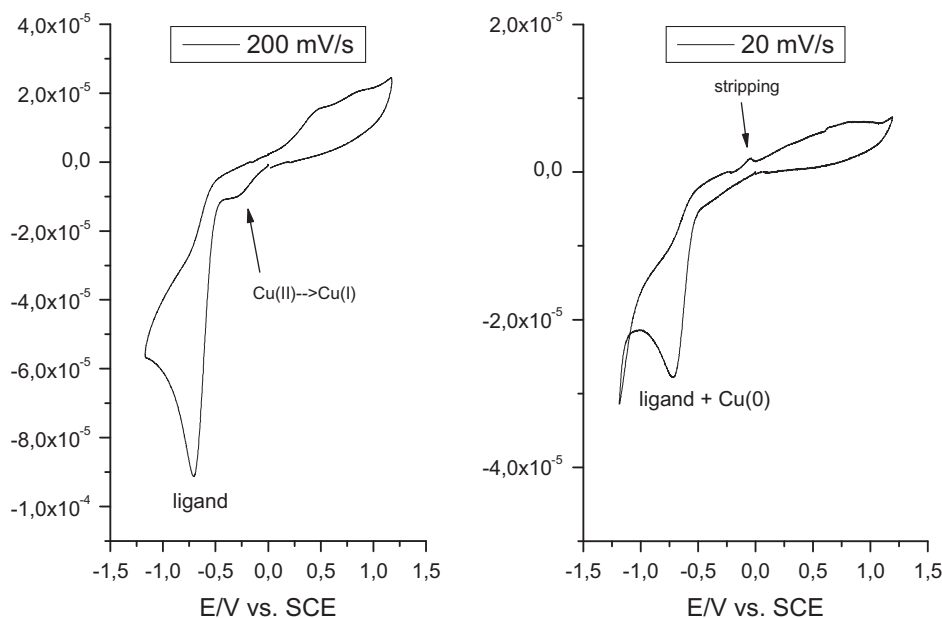


Fig. 6. Cyclic voltammetry curves of the complex at two different scan rate: 0.02 and 0.2 V/s, obtained in 0.1 M acetate buffer (pH 4.4) and using Glassy Carbon electrode as working electrode, Pt counter electrode, and SCE as reference. Temperature: 25 °C.

Table 3

$E_{1/2}$ (V vs. SCE) of the free ligand L^{MN} and the related Cu(II) complex $\{[(L^{MN})_2Cu]Cl_2\}$ and at different buffered pHs, and E_{pc} of the (V vs. SCE) of Cu(II)/complex concerning the Cu(II)/Cu(I) reduction. Scan rate 0.05 V/s.

	pH 4	pH 8
$L^{MN} E_{1/2}$	−0.571	−0.726
$\{[(L^{MN})_2Cu]Cl_2\} E_{1/2}$	−0.609	−0.647
$\{[(L^{MN})_2Cu]Cl_2\} E_{pc}$	−0.36	−0.47

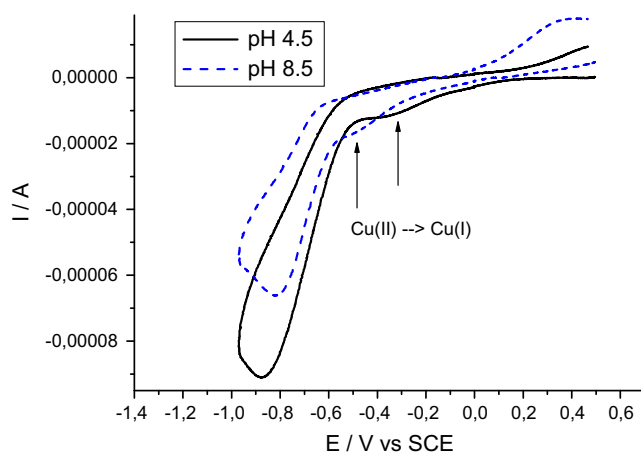


Fig. 7. Comparison of the CV curves of $\{[(L^{MN})_2Cu]Cl_2\}$ at two different pHs: 4.4 and 8.5. Glassy Carbon electrode as working electrode, Pt counter electrode, and SCE as reference. Temperature: 25 °C. Scan rate: 0.05 V/s.

edge for structural considerations.

3.3. Cyclic voltammetry

The electroreduction properties of the copper(II) complex $\{[(L^{MN})_2Cu]Cl_2\}$ has been tested and the typical cyclic voltammograms at two selected scan rate are reported in Fig. 6, using a Glassy Carbon (GC) working electrode. The curve recorded at 200 mV/s (left) displays several set of reduction and oxidation phenomena which are indicated in the figure, most of them being irreversible or quasi reversible. Generally, we report that the reduction of the Cu(II) in the studied complexes is rather difficult and happens at lower potential than those observed for Cu(II) complexes in tetrahedral coordination [61]. This has been also recently observed for Cu(II) on a quasi-octahedral environment respect to square planar Cu(II) core [62]. As a consequence, the observed Cu(II) reduction appears at potential close to that of the ligand, which appears at about −0.9 V versus SCE (E cathodic peak). Cyclic voltammetric test on solutions of the free ligand has confirmed this value of the reduction potential (see Supplementary Information).

Peaks in the anodic direction are related to the subsequent oxidation of the ligand. When low scan rate is used to test the electrochemical behaviour, the electronic charge furnished to the system is also used for the formation of Cu(0) at the electrode surface, and hence a typical ‘stripping’ peak is observed in the back scan at potential close to 0 versus SCE. The Cu(0) formation during reduction appears at potential close to the ligand reduction. Table 3 summarizes the reduction potential (peak) of the ligand as well as the complex at different pH values.

Fig. 7 displays the electrochemical behaviour (reduction) of the Cu(II) complex at two different pHs, basic and acidic, recorded at 50 mV/s. The curves appear similar to the one of Fig. 6, but, interestingly, the reduction of the Cu(II) to the Cu(I) is pH dependent, with

the acidic media making the reduction more easy. In fact, a positive shift of about 100 mV is observed for E_{pc} at pH 4.5 respect to 8.5.

4. Discussion

Unravelling the molecular structure of metal complexes in solution is typically a difficult task, even while using an appropriate probe for solutions as the X-ray absorption spectroscopy does. One of the main limitation in EXAFS is the small backscattering power of light elements which surround a central atom, which becomes even worse in structural studies in solutions. However, we have observed that the $\{[(L^{MN})_2Cu]Cl_2\}$ complex studied in this paper, which also displays interesting anticancer properties, is structurally stable in solutions, as the FT curves observed in Fig. 3 proves. This structural stability help reducing the static structural disorder (similar atomic configurations like the atoms constituent the pyrazolyl ring scatter in the same fashion) and adds more experimental signals which, in turns, means that the first atomic shell could be probed efficiently, even considering the modest scattering of the lights elements. The fact that the complex remains stable in solution is confirmed by the structural information reported in Table 2, which indicates the same bond distances of the equatorial Cu–N bonds (with coordination of 4, two per ligand) in the powder and in aqueous solution at different pH values. A more interesting trend is observed in the case of the Cu–O axial interaction. The occurrence of this interaction has been confirmed by a separate fitting procedure aimed to verify both the coordination number and the Cu–O bond distances (see Supplementary Materials). The outcome has indicated the necessity of this Cu–O inclusion in all fitting procedures of the solutions. Concerning this bond, we have observed that the lower the pH the lengthening of the bond. At moderate alkaline solution this bond is 2.29 Å which becomes 2.38 Å if the pH is about 4.5. This structural modification is large, and can be connected to the XANES spectra, which display an increase of the pre-edge peak A of Fig. 5, being the highest at acidic pH. This peak becomes higher when deviation from a centrosymmetry is observed in an octahedral environment [63], and this occurs at acidic pH, as indicated in Table 2.

Structurally, when the Cu–O interaction lengthens at lower pH, there should be less donor charge to the Cu from the oxygen atoms with respect to the metal core detected at pH 8.5, and in fact a very small negative shift of the pre-edge peak A (about 0.3 eV) is also observed in the inset of Fig. 5, confirming that copper is slightly electropositive at pH 4.5 with respect to pH 8.5. This picture also matches well to the electrochemical experiments. In fact, as showed in Fig. 6, the reduction of the Cu(II) complex is pH dependent, and the acidic media makes the reduction of the Cu(II)/Cu(I) redox couple easiest: the Cu(II)/Cu(I) couple is more electropositive as its potential shifts 100 mV to more positive potential.

The stability of $\{[(L^{MN})_2Cu]Cl_2\}$ complex in solution is also observed by inspection of the EXAFS bond variances, which are similar. This observation, coupled to the invariance (or slightly difference) of the Cu–N equatorial bonds and the fixed Cu–N–C and Cu–N–N angles, makes the distances from the central atom (Cu) to the various atoms of the pyrazolyl rings rather similar, as evidenced at the bottom of Table 2, adding new findings concerning the stability issue.

From the CV curves, not only the irreversibility of the Cu(II)/Cu(I) system but also the relative potential of the E_{pc} respect to the values observed for the Cu(II) complexes in tetrahedral coordination [61], suggests a quasi-octahedral coordination of $\{[(L^{MN})_2Cu]Cl_2\}$ in the studied solutions. This has been recently observed in the literature [62]. The irreversibility of the Cu(II)/Cu(I) system is due to the coordination geometry for $\{[(L^{MN})_2Cu]Cl_2\}$ in the Cu(II) oxidation state (quasi-octahedral), which differs from the preferred

orientation for Cu(I) (a tetrahedral one). In fact, Cu(II) complexes with tetrahedral or square planar coordination are characterized by reversible peaks in their cyclic voltammetry, because the Cu(II) reduction does not involve structural rearrangements [62].

5. Conclusions

A joint EXAFS and XANES study has been conducted to reveal the solution structure (at three different pHs) of the $\{[L^{MN}]_2\text{-Cu}(\text{Cl}_2)\}$ complex with known anticancer activity. The study has evidenced a relevant multiple scattering contribution, even in solution, allowing to check the local environment of the copper centre. The Cu(II) complex results stable upon dissolution in aqueous solution, and the copper centre is found to be coordinated by two molecules of ligands, describing a quasi-octahedral environment in all the investigated solutions. The four equatorial Cu–N bond distances remain unchanged in the different pH buffers (no pH dependence), whereas Cu–O bond distance lengthens at acidic pH. XANES spectra have evidenced a change of the local octahedral symmetry around the Cu site at pH 4.4, suggesting a more tetragonal distortion at this pH value. XANES also indicated a slightly electropositive Cu at pH 4.4 with respect to pH 8.5, as suggested by the Cu edge features. These findings agree with the cyclic voltammetry study which indicated a positive shift of about 100 mV for the Cu(II)/Cu(I) redox couple at acid pH.

Acknowledgments

Thanks are due to RFO funding from the University of Bologna. XAS measurements at ELETTRA were supported by Sincrotrone Trieste S.C.p.A. (Proposal No. 20090307). We are grateful to Sano-fi-Aventis S.p.A. and CIRCMSB (Consorzio Interuniversitario di Ricerca in Chimica dei Metalli nei Sistemi Biologici).

Appendix A. Supplementary data

Supplementary data associated with this article can be found, in the online version, at <http://dx.doi.org/10.1016/j.poly.2012.08.073>.

References

- [1] H.R. Bigmore, S.C. Lawrence, P. Mountford, C.S. Tredget, *Dalton Trans.* (2005) 635.
- [2] A. Otero, A. Lara-Sanchez, J. Fernandez-Baeza, E. Martinez-Caballero, I. Marquez-Segovia, C. Alonso-Moreno, L.F. Sanchez-Barba, A.M. Rodriguez, I. Lopez-Solera, *Dalton Trans.* 39 (2010) 930.
- [3] S. Trofimenko, *Scorpionates: The Coordination Chemistry of Poly(pyrazolyl)borate Ligands*, Imperial College Press, London, 1999.
- [4] C. Santini, M. Pellei, G. Gioia Lobbia, G. Papini, *Mini-Rev. Org. Chem.* 7 (2010) 84.
- [5] M. Pellei, G. Gioia Lobbia, G. Papini, C. Santini, *Mini-Rev. Org. Chem.* 7 (2010) 173.
- [6] A. Otero, J. Fernandez-Baeza, A. Antinolo, J. Tejada, A. Lara-Sanchez, L. Sanchez-Barba, M. Sanchez-Molina, S. Franco, I. Lopez-Solera, A.M. Rodriguez, *Eur. J. Inorg. Chem.* (2006) 707.
- [7] A. Otero, J. Fernandez-Baeza, A. Antinolo, J. Tejada, A. Lara-Sanchez, L. Sanchez-Barba, M. Sanchez-Molina, S. Franco, I. Lopez-Solera, A.M. Rodriguez, *Dalton Trans.* (2006) 4359.
- [8] N. Burzlaff, I. Hegelmann, B. Weibert, *J. Organomet. Chem.* 626 (2001) 16.
- [9] A. Beck, B. Weibert, N. Burzlaff, *Eur. J. Inorg. Chem.* (2001) 521.
- [10] E. Huebner, T. Haas, N. Burzlaff, *Eur. J. Inorg. Chem.* (2006) 4989.
- [11] P.C.A. Bruijninx, I.L.C. Buurmans, S. Gosiewska, M.A.H. Moelands, M. Lutz, A.L. Spek, G. van Koten, R.J.M. Klein Gebbink, *Chem. Eur. J.* 14 (2008) 1228.
- [12] E. Galaron, M. Giorgi, I. Artaud, *Dalton Trans.* (2007) 1047.
- [13] T.C. Higgs, C.J. Carrano, *Inorg. Chem.* 36 (1997) 291.
- [14] T.C. Higgs, C.J. Carrano, *Inorg. Chem.* 36 (1997) 298.
- [15] C. Santini, M. Pellei, *Curr. Bioact. Compd.* 5 (2009) 243.
- [16] N.V. Fischer, G. Türkoglu, N. Burzlaff, *Curr. Bioact. Compd.* 5 (2009) 277.
- [17] B.S. Hammes, C.J. Carrano, *Chem. Commun.* (2000) 1635.
- [18] M. Pellei, G. Gioia Lobbia, C. Santini, R. Spagna, M. Camalli, D. Fedeli, G. Falcioni, *Dalton Trans.* (2004) 2822.
- [19] C. Marzano, M. Pellei, D. Colavito, S. Alidori, G. Gioia Lobbia, V. Gandin, F. Tisato, C. Santini, *J. Med. Chem.* 49 (2006) 7317.
- [20] M. Pellei, G. Gioia Lobbia, M. Ricciutelli, C. Santini, *J. Coord. Chem.* 58 (2005) 409.
- [21] F. Benetollo, G. Gioia Lobbia, M. Mancini, M. Pellei, C. Santini, *J. Organomet. Chem.* 690 (2005) 1994.
- [22] F. Marchetti, M. Pellei, C. Pettinari, R. Pettinari, E. Rivarola, C. Santini, B.W. Skelton, A.H. White, *J. Organomet. Chem.* 690 (2005) 1878.
- [23] M. Pellei, C. Santini, M. Mancini, S. Alidori, M. Camalli, R. Spagna, *Polyhedron* 24 (2005) 995.
- [24] M. Porchia, G. Papini, C. Santini, G. Gioia Lobbia, M. Pellei, F. Tisato, G. Bandoli, A. Dolmella, *Inorg. Chim. Acta* 359 (2006) 2501.
- [25] M. Pellei, S. Alidori, M. Camalli, G. Campi, G. Gioia Lobbia, M. Mancini, G. Papini, R. Spagna, C. Santini, *Inorg. Chim. Acta* 361 (2008) 1456.
- [26] M. Giorgetti, L. Guadagnini, S.G. Fiddy, C. Santini, M. Pellei, *Polyhedron* 28 (2009) 3600.
- [27] C. Pettinari, A. Cingolani, G. Gioia Lobbia, F. Marchetti, D. Martini, M. Pellei, R. Pettinari, C. Santini, *Polyhedron* 23 (2004) 451.
- [28] G. Gioia Lobbia, M. Pellei, C. Pettinari, C. Santini, B.W. Skelton, N. Somers, A.H. White, *J. Chem. Soc., Dalton Trans.* (2002) 2333.
- [29] S. Alidori, G. Gioia Lobbia, G. Papini, M. Pellei, M. Porchia, F. Refosco, F. Tisato, S. Lewis Jason, C. Santini, *J. Biol. Inorg. Chem.* 13 (2008) 307.
- [30] M.P. Hay, W.R. Wilson, J.W. Moselen, B.D. Palmer, W.A. Denny, *J. Med. Chem.* 37 (1994) 381.
- [31] A. Brecia, B. Cavalleri, G.E. Adams, *Nitroimidazoles, Chemistry, Pharmacology and Clinical Application*, Plenum, New York, 1982.
- [32] W.J. Koh, K.S. Bergman, J.S. Rasey, L.M. Peterson, M.L. Evans, M.M. Graham, J.R. Grierson, K.L. Lindsley, T.K. Lewellen, K.A. Krohn, *Int. J. Radiat. Oncol. Biol. Phys.* 33 (1995) 391.
- [33] G.V. Martin, J.H. Caldwell, M.M. Graham, J.R. Grierson, K. Kroll, M.J. Cowan, T.K. Lewellen, J.S. Rasey, J.J. Casciari, K.A. Krohn, *J. Nucl. Med.* 33 (1992) 2202.
- [34] A. Nunn, K. Linder, H.W. Strauss, *Eur. J. Nucl. Med.* 22 (1995) 265.
- [35] S.J. Read, T. Hirano, D.F. Abbott, J.I. Sachinidis, H.J. Tochon-Danguy, J.G. Chan, G.F. Egan, A.M. Scott, C.F. Bladin, W.J. McKay, G.A. Donnan, *Neurology* 51 (1998) 1617.
- [36] E.L. Engelhardt, R.F. Schneider, S.H. Seeholzer, C.C. Stobbe, J.D. Chapman, *J. Nucl. Med.* 43 (2002) 837.
- [37] Z. Li, T. Chu, X. Liu, X. Wang, *Nucl. Med. Biol.* 32 (2005) 225.
- [38] P.D. Bonnitcha, S.R. Bayly, M.B.M. Theobald, H.M. Betts, J.S. Lewis, J.R. Dilworth, *J. Inorg. Biochem.* 104 (2010) 126.
- [39] M. Pellei, G. Papini, A. Trasatti, M. Giorgetti, D. Tonelli, M. Minicucci, C. Marzano, V. Gandin, G. Aquilanti, A. Dolmella, C. Santini, *Dalton Trans.* 40 (2011) 9877.
- [40] A. Filippini, *J. Phys.: Condens. Matter* 13 (2001) R23.
- [41] M. Giorgetti, M. Berrettoni, W.H. Smyrl, *Chem. Mater.* 19 (2007) 5991.
- [42] P. D'Angelo, M. Benfatto, S. Della Longa, N.V. Pavel, *Phys. Rev. B: Condens. Matter Mater. Phys.* 66 (2002) 0642091.
- [43] I. Ascone, A. Cognigni, M. Giorgetti, M. Berrettoni, S. Zamponi, R. Marassi, *J. Synchrotron Radiat.* 6 (1999) 384.
- [44] M. Tromp, J.A. Van Bokhoven, A.M. Arink, J.H. Bitter, G. Van Koten, D.C. Koningsberger, *Chem. Eur. J.* 8 (2002) 5667.
- [45] P. Frank, M. Benfatto, R.K. Szilagy, P. D'Angelo, S. Della Longa, K.O. Hodgson, *Inorg. Chem.* 44 (2005) 1922.
- [46] P. Cecchi, M. Berrettoni, M. Giorgetti, G. Gioia Lobbia, S. Calogero, L. Stievano, *Inorg. Chim. Acta* 318 (2001) 67.
- [47] M. Giorgetti, M. Pellei, G. Gioia Lobbia, C. Santini, *J. Phys.: Conf. Ser.* 190 (2009) 012146.
- [48] G. Aquilanti, M. Giorgetti, M. Minicucci, G. Papini, M. Pellei, M. Tegoni, A. Trasatti, C. Santini, *Dalton Trans.* 40 (2011) 2764.
- [49] A. Di Cicco, G. Aquilanti, M. Minicucci, E. Principi, N. Novello, A. Cognigni, L. Olivi, *J. Phys.: Conf. Ser.* (2009) 190.
- [50] A. Filippini, A. Di Cicco, *Phys. Rev. B: Condens. Matter* 52 (1995) 15135.
- [51] A. Filippini, A. DiCicco, C.R. Natoli, *Phys. Rev. B* 52 (1995) 15122.
- [52] M. Giorgetti, M. Berrettoni, A. Filippini, P.J. Kulesza, R. Marassi, *Chem. Phys. Lett.* 275 (1997) 108.
- [53] L. Hedn, B.I. Lundqvist, *J. Phys. C: Solid State Phys.* 4 (1971) 2064.
- [54] M.O. Krause, J.H. Oliver, *J. Phys. Chem. Ref. Data* 8 (1979) 329.
- [55] T. Yamamoto, *X-Ray Spectrom.* 37 (2008) 572.
- [56] L.S. Kau, D.J. Spira-Solomon, J.E. Penner-Hahn, K.O. Hodgson, E.I. Solomon, *J. Am. Chem. Soc.* 109 (1987) 6433.
- [57] J.L. DuBois, P. Mukherjee, T.D.P. Stack, B. Hedman, E.I. Solomon, K.O. Hodgson, *J. Am. Chem. Soc.* 122 (2000) 5775.
- [58] S.E. Shadle, J.E. Penner-Hahn, H.J. Schugar, B. Hedman, K.O. Hodgson, E.I. Solomon, *J. Am. Chem. Soc.* 115 (1993) 767.
- [59] J. Chaboy, A. Munoz-Paez, F. Carrera, P. Merklung, E.S. Marcos, *Phys. Rev. B: Condens. Matter Mater. Phys.* 71 (2005) 134208/1.
- [60] J. Chaboy, A. Munoz-Paez, E.S. Marcos, *J. Synchrotron Radiat.* 13 (2006) 471.
- [61] P. Zanello, *Inorganic Electrochemistry: Theory, Practice and Application*, second ed., Royal Society of Chemistry, Cambridge, 2003. pp. 302–314.
- [62] L.I. Vagliasindi, G. Arena, R.P. Bonomo, G. Pappalardo, G. Tabbi, *Dalton Trans.* 40 (2011) 2441.
- [63] I.J. Pickering, G.N. George, C.T. Dameron, B. Kurz, D.R. Winge, I.G. Dance, *J. Am. Chem. Soc.* 115 (1993) 9498.